Supplementary Files

Supplementary Materials and Methods

Supplementary Figure 1.

Supporting Figure 1. *MIR142* mutations attenuate miR-142-3p and miR-142-5p functions.

Supplementary Figure 2.

Supporting Figure 2. *Mir142* loss alters differentiation in mature hematopoietic populations.

Supplementary Figure 3.

Supporting Figure 3. *Mir142* loss alters differentiation in MPPs and HSCs.

Supplementary Figure 4.

Supporting Figure 4. *Mir142*$^{-/-}$ bone marrow exhibits reduced repopulating activity with a loss of HSC lymphoid potential.

Supplementary Figure 5.

Supporting Figure 7. *Mir142* loss enhances *IDH2*^{R172K} disease initiating capacity.

Supplementary Materials and Methods

Antibodies

The following antibodies were used for Western blotting and/or Chromatin immunoprecipitation assays: H3K4me3 (Thermo Fisher, 07-473-MI), H3K36me2 (Active Motif, 39255), H3K36me3 (Abcam, ab9050), H3K27me3 (Fisher, 07449MI), total H3 (Abcam, ab1791), ASH1L (Santa Cruz, sc-98301), and β-actin (Sigma, AC-74).

Flow cytometry was performed with the following murine antibodies (eBioscience unless otherwise noted): Ly-6C/G (RB6-8C5, Gr-1), Ly-6A/E (D7, Sca1), CD3e (145-2C11), CD16/32 (93, Fc 2R/ Fc 3R), CD34 (RAM34), CD41 (MWReg30), CD45R (RA3-6B2, B220), CD45.1 (A20, Ly5.1), CD45.2 (104, Ly5.2), CD48 (HM48-1), CD71 (Bio-Rad, YTA74.4, TfR1), CD117 (2B8, c-kit), CD135 (A2F10, Flt3), CD150 (Biolegend, TC15-12F12.2, SLAM), CD229 (Biolegend, Ly9ab3, Ly-9), TER-119 (Ter-119), CD44 (Fisher, IM7) and the following human antibodies (eBioscience unless otherwise noted): CD9 (BD Biosciences, M-L13), CD14 (61D3), CD15 (Fisher, HI98), CD16 (3G8), CD34 (PE-pool, Beckman Coulter Genomics, PN IM1459U), and CD45 (BD Biosciences, H130).

AutoMACs cell separation was performed with the following antibodies: CD117 microbeads, murine (Miltenyi, Cat# 130-091-224) and CD34 microbeads, human indirect kit (Miltenyi, Cat# 130-046-701).

RISC immunoprecipitation was performed with the following antibodies: Anti-pan Ago (Millipore, 2A8) and AffiniPure Rabbit anti-mouse IgG (Jackson Immunoresearch, 315-005-008) on protein A dynabeads (Thermo Fisher, Cat # 10001D).

Flow cytometry

Cells were stained by standard protocols. Flow cytometry data were collected on a Gallios 10-color, 4-laser flow cytometer (Beckman Coulter) and analyzed with FlowJo software (Treestar).

Cell sorting was performed with a modified Beckman Coulter MoFlo or a Sony SY3200 Synergy cell sorter.

Quantitative PCR

Gene expression via reverse transcriptase-quantitative PCR was determined with the following Taqman assays (Thermo Fisher): Hoxa9 (Mm00439364_m1), Hoxa10 (Mm00433966_m1), Ash1l (Mm00467322_m1), Mir142-5p (Mmu481324_mir), Actb (Mm04394036_g1), SnoRNA202 (ID# 001232), and GAPDH (Hs02758991_g1).

Quantification and statistical analysis

Analysis and quantification of flow cytometry data were performed using FlowJo software (Tree Star). Analysis and quantification of Western blots were performed with the ChemiDoc MP system (Bio-Rad) using Image Lab 6.0 software (Bio-Rad). RT-qPCR data acquisition and analysis were performed with a StepOnePlus (Thermo Fisher). Acquisition and analysis of luciferase activity were performed with a Synergy H1 Hybrid Reader (Biotek). Statistical analysis was done using GraphPad Prism 6 with the specific analytic tests performed detailed in the appropriate figure legends. Unless otherwise noted, data is represented as the mean ± the standard error of the mean.

Luciferase assays

The 3' UTRs of *RAC1*, *TGFBR1*, and *ASH1L* were cloned into the psiCHEK-2 luciferase vector (Promega). For MIR142 overexpression, wild type or mutant MIR142 hairpins were inserted, with flanking genomic sequences, into the 3' UTR of GFP in a lentiviral HIV- MND-IRES-GFP vector. Using Lipofectamine 2000, plasmids were co-transfected into HEK293T cells. 48 hours post-transfection, luciferase activity was measured using the Dual-Glo system (Promega) and a

Synergy H1 Hybrid Reader. Data represent the ratio of experimental (Renilla) to control (Firefly) luciferase.

Isolation of human hematopoietic populations

$CD34^+$ cells were isolated from healthy donor bone marrow using the MACS indirect CD34 MicroBead Kit (130-046-701) on the autoMACS Pro Separator (Miltenyi) per manufacturer's protocol. Myeloid blasts from AML bone marrow samples with < 70% blasts were sorted directly into Trizol LS (Thermo Fisher). AML blasts were identified as $CD34^+CD45^{dim}$ cells; in cases where the AML was not $CD34^+$, $CD45^{dim}SS^{lo}FS^{hi}$ cells were identified as blasts. RNA was isolated from Trizol LS per the manufacturer's protocol.

Small RNA library generation and sequencing

cDNA was generated from RNA derived from either AML samples (500 ng input) or healthy donor hematopoietic populations (100 ng input) using the NEBNext Small RNA Prep Set for Illumina (New England Biolabs). The LabChipXT DNA 750 fractionation system (PerkinElmer) was used to isolate cDNA derived from RNA molecules 17-75 nucleotides in size. Small RNA cDNA libraries were run with one sample per lane on an Illumina GAIIX or with multiple samples multiplexed per lane on an Illumina HiSeq2000.

Small RNA bioinformatics pipeline

Sequencing reads were trimmed to remove the 3' adaptor sequence prior to using the Burrows-Wheeler Aligner (1) to map reads against the human reference genome. Post alignment downstream analysis included splitting the aligned BAM files into bins based on read length. "Clusters" were defined as regions of contiguous read coverage and were interrogated against known annotation databases including miRBase, Biomart5, Genbank6, Ensembl7, and an in-house annotation database. Alignments across all samples were merged to generate a "Common

Cluster" annotation list, representing a comprehensive set of annotated and novel regions for cross-sample comparison. Reads for miR-142-5p and miR-142-3p were normalized to the total number of mapped reads 17-75 nucleotides in length.

RISC immunoprecipitation

Plasmids expressing either mutant or wild type MIR142 hairpins were constructed as described previously and transfected into HEK293T cells with Lipofectamine 2000. Immunoprecipitation was performed 48 hours post-transfection.

To measure cellular levels of MIR142-5p and MIR142-3p, RNA was isolated from total cells with Trizol LS (Thermo Fisher). Small RNA library generation and sequencing was then performed as previously described. To determine cellular levels of precursor MIR142, Trizol LS extracted RNA was treated with the Turbo DNA-free Kit (Thermo Fisher). cDNA was then made with the High-Capacity cDNA Reverse Transcription Kit (Thermo Fisher). Precursor MIR142 levels were determined using PowerUP SYBR Green (Thermo Fisher), 5' primer CAC AGT ACA CTC ATC CAT AAA GTA GG, and 3' primer GAA AGC ACT ACT AAC AGC ACT GGA. Precursor MIR142 levels are relative to that of *GAPDH* expression.

To measure levels of RISC-associated MIR142-5p and MIR142-3p, 100 μl of protein A dynabeads were incubated with a bridging anti-mouse IgG antibody for 1 hour at room temperature followed by labeling with a pan anti-Ago antibody for 4 hours at 4°C. Transfected cells were pelleted and lysed with lysis buffer [0.1% sodium dodecyl sulfate (Sigma), 0.5 % deoxycholic acid (Sigma), 0.5 % Tergitol (Sigma), RNAsin (Promega), and a protease inhibitor cocktail (Sigma) in PBS]. Following centrifugation at 15,000 rpm at 4°C for 1 hour, the cell lysate was added to the labeled beads and incubated for 2 hours at 4°C. The beads were washed with lysis buffer in PBS, lysis buffer in 5X PBS, and PBS. The beads were resuspended in Trizol (Thermo Fisher) and incubated for 5 minutes at room temperature to dissociate the RNA, which was then extracted per manufacturer's protocol.

Chromatin immunoprecipitation (ChIP)

Bone marrow c-kit^{+}-selected cells were isolated with CD117 MicroBeads on the autoMACS Pro Separator. ChIP was performed with the LowCell# ChIP kit (Diagenode). Briefly, cells were incubated in 1% formaldehyde (Amresco) on ice to cross-link DNA with histones. After ten minutes, glycine was added to stop cross-linking. Chromatin was sheared with a Covaris E210 (140.0 peak power, 10.0% duty factor, 200 cycles/burst, 10 minutes) and incubated at 4°C overnight with antibodies against H3K4me3, H3K36me2 or H3K36me3 on Protein A dynabeads. Cross-linking was reversed and DNA isolated with the IPure kit V2 (Diagenode), DNA precipitant (Diagenode), and DNA co-precipitant (Diagenode). Quantitative PCR was performed with PowerUP SYBR Green (Thermo Fisher) using previously described primers targeting the *Hoxa9* and *Actb* promoter regions (2). DNA pulled down via immunoprecipitation was normalized to input DNA.

Supplementary References

1. Li H, and Durbin R. Fast and accurate short read alignment with Burrows-Wheeler transform. *Bioinformatics.* 2009;25(14):1754-60.
2. Zhu L, Li Q, Wong SH, Huang M, Klein BJ, Shen J, Ikenouye L, Onishi M, Schneidawind D, Buechele C, et al. ASH1L Links Histone H3 Lysine 36 Dimethylation to MLL Leukemia. *Cancer Discov.* 2016;6(7):770-83.

Supplementary Figure 1

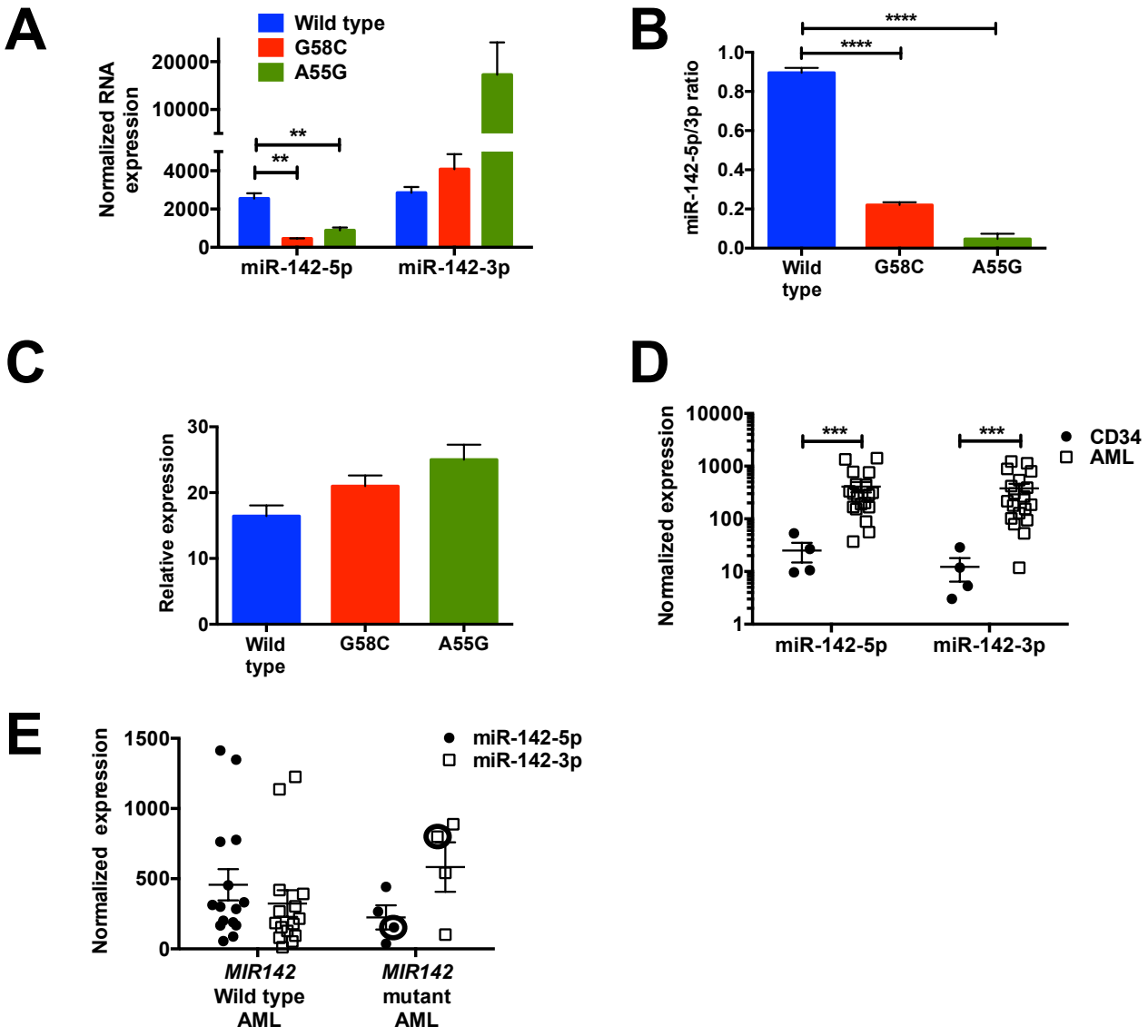

Supplementary Figure 1

a-b, Total level (**a**) and ratio (**b**) of mature cellular miR-142-5p and miR-142-3p transcripts after overexpression of the wild type MIR142 hairpin (n=3) or its G58C (n=3) and A55G (n=3) mutants. **c,** Precursor MIR142 hairpin expression after overexpression of the wild type or mutant MIR142 hairpins. Expression is relative to *GAPDH*. **d,** MiR-142-5p and miR-142-3p expression in normal $CD34^{+}$ progenitors versus AML cells. **e,** Total level of mature miR-142-5p and miR-142-3p in AML cells either with or without *MIR142* mutations. For **a** and **d**-**e** normalized expression was defined as (number of reads mapped to a gene/total number of reads) x 10^{6}. For **a**-**b**, significance was determined with an unpaired t test. For **d**, significance was determined with a Mann-Whitney test. **P<0.01; ***P<0.001; ****P<0.0001.

Supplementary Figure 2

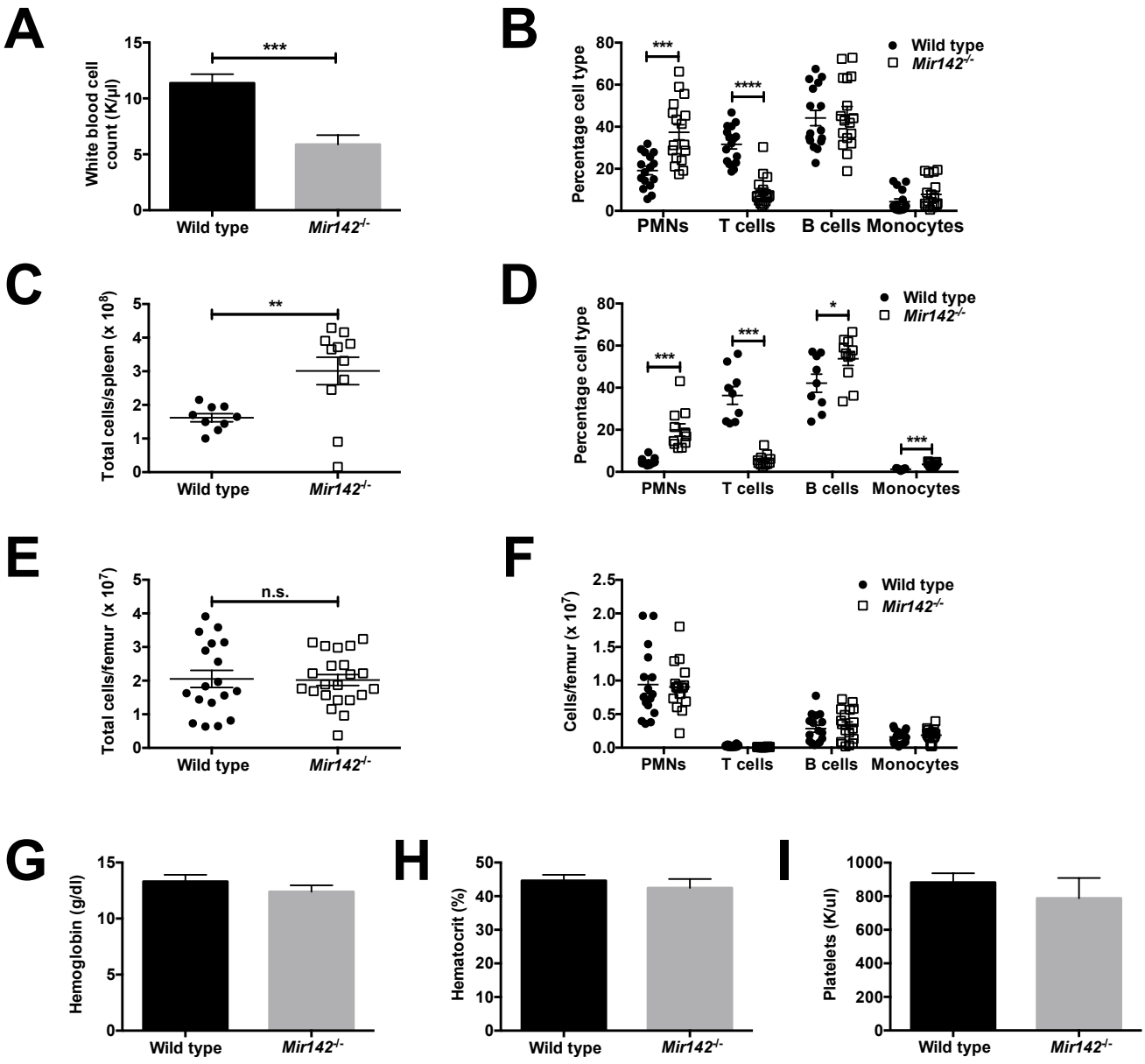

Supplementary Figure 2

a, White blood cell count in *Mir142*$^{-/-}$ mice (n=10) compared to wild type (n=9). **b,** Percentage of mature hematopoietic cell types in the peripheral blood. **c,** Spleen cellularity. **d,** Percentage of mature hematopoietic cell types in the spleen. **e,** Number of bone marrow cells per femur. **f,** Total number of mature hematopoietic cell types per femur. **g-i**, Hemoglobin (**g**), hematocrit (**h**), and platelet counts (**i**) in the peripheral blood of *Mir142*$^{-/-}$ (n=10) and wild type (n=9) mice. Significance was determined with an unpaired t test. n.s. not significant. *P<0.05; **P<0.01; ***P<0.001; ****P<0.0001.

Supplementary Figure 3

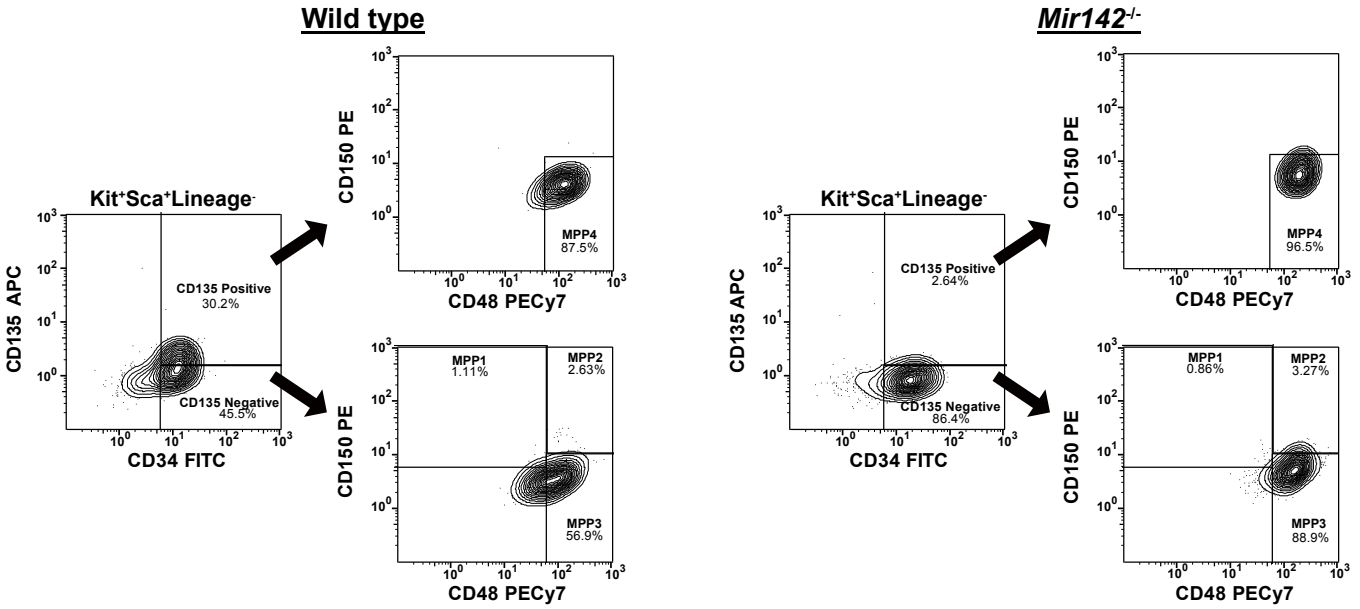

Supplementary Figure 3
Representative flow plots showing the gating strategy used to quantify multipotent progenitor cell populations. Data in the first flow plot are gated on KSL cells.

Supplementary Figure 4

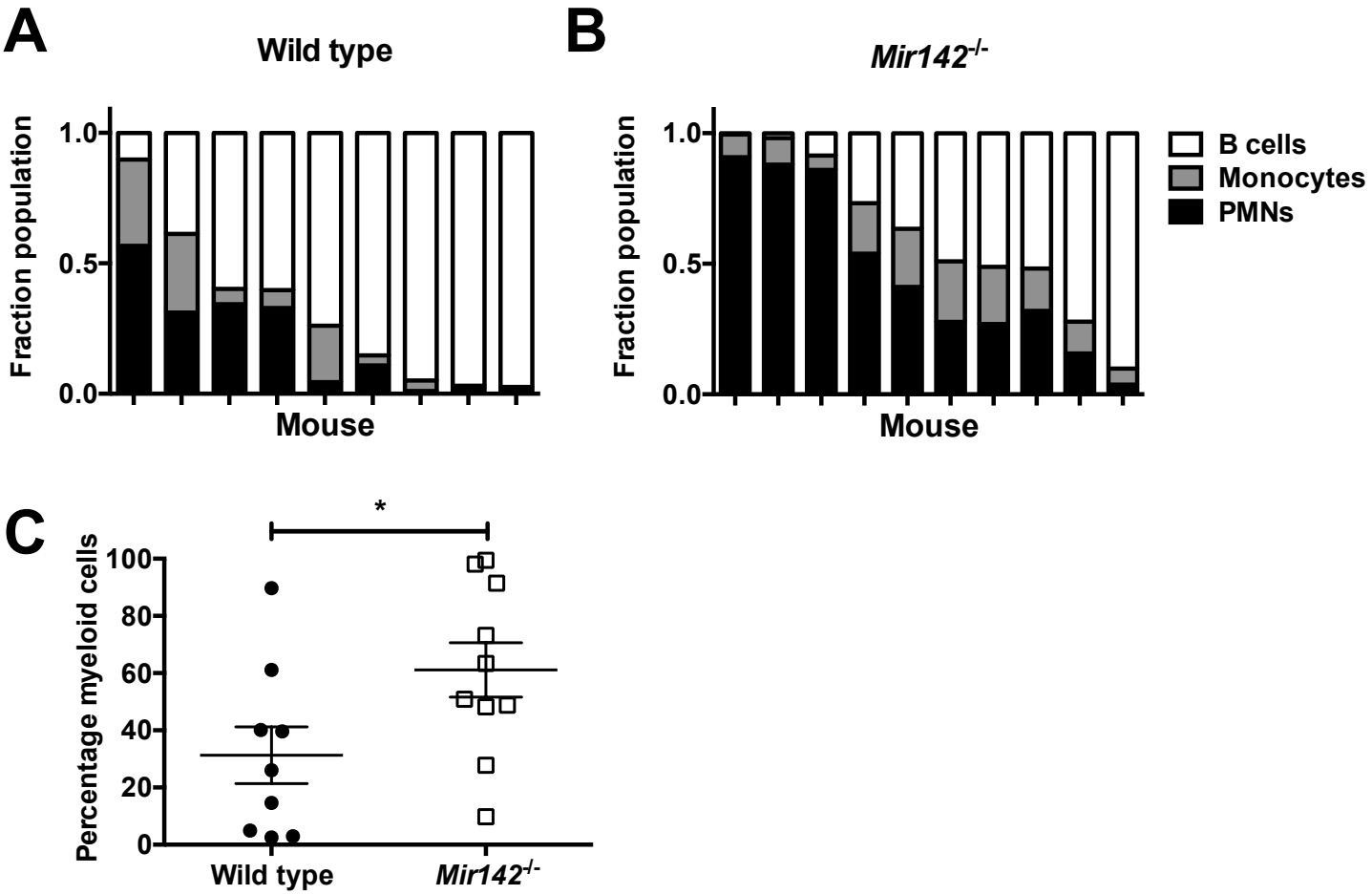

Supplementary Figure 4

a-b, Contribution of the indicated hematopoietic lineage excluding T cells (i.e. $Gr1^+$, $CD115^+$, or $B220^+$ cells) to the total donor leukocyte pool in the peripheral blood of mice transplanted with wild type (**a**) or *Mir142*$^{-/-}$ (**b**) $CD150^+CD48^-KSL$ cells 24 weeks following transplantation. Recipient mice were included in this analysis if they had identifiable donor engraftment in both myeloid ($Gr1^+$ or $CD115^+$) and lymphoid ($B220^+$ or $CD3^+$) lineages. **c**, Percentage of cells in **a** or **b** that were myeloid (i.e. $Gr1^+$ or $CD115^+$). Significance was determined with an unpaired t test. *P<0.05.

Supplementary Figure 5

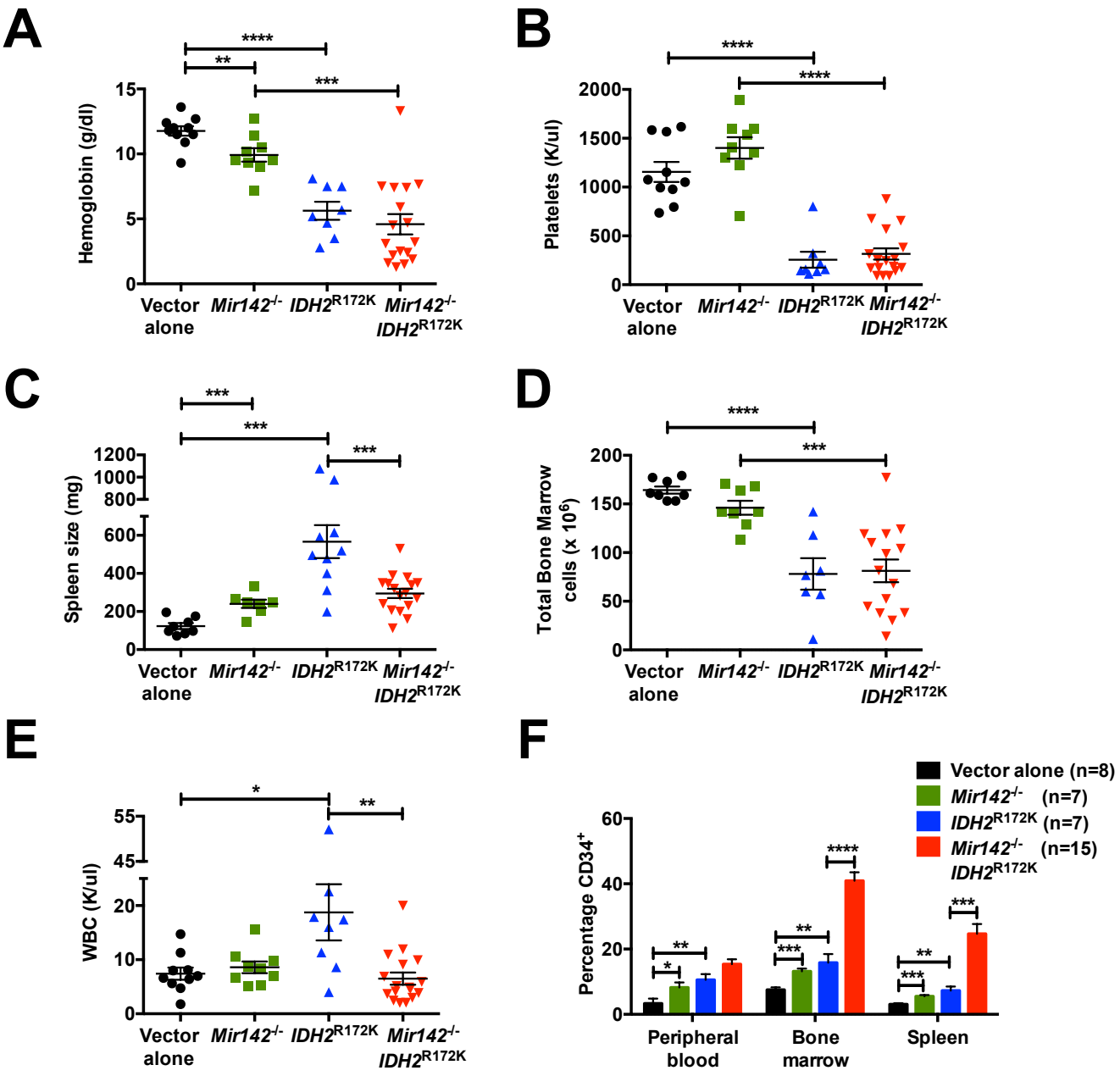

Supplementary Figure 5

a-f, Mice were transplanted with wild type bone marrow c-kit^{+} cells transduced with an empty retrovirus (vector alone) or retrovirus expressing *IDH2*^{R172K} or with *Mir142*$^{-/-}$ c-kit^{+} cells transduced with empty retrovirus (*Mir142*$^{-/-}$) or *IDH2*^{R172K} retrovirus. Shown are the hemoglobin (**a**), platelet count (**b**), spleen size (**c**), total bone marrow cell number from two femurs, tibias, and pelvises (**d**), white blood cell count (**e**), and percentage of CD34^{+} cells (**f**) upon sacrifice. Significance was determined with an unpaired t test. *P<0.05; **P<0.01 ***P<0.001; ****P<0.0001.